Materials Transactions, Vol. 48, No. 9 (2007) pp. 2476 to 2482

A Scheme to Design Multi-Component Bulk Metallic Glasses in *Ideal* Glass-Forming Liquids

Z. P. Lu[1,2,*] and C. T. Liu[3]

[1]*State Key Laboratory for Advanced Metals and Materials, University of Science and Technology Beijing, Beijing, China 100083*
[2]*Meterials Science and Technology Division, Oak Ridge National Laboratory, Oak Ridge, TN 37831-6115, USA*
[3]*The University of Tennessee, Department of Materials Science and Engineering, Knoxville, TN 37996-2200, USA*

In this study, we have proposed to use binary eutectics, rather than individual constituent elements, as basic units for designing complex multi-component bulk metallic glasses (BMGs), based on a novel physical concept of "*ideal*" glass-forming liquids. An innovative approach to designing multi-component BMGs in these ideal liquids was thus established and the reliability and usefulness of the current approach of this strategy has been confirmed in the Zr-Fe-Cu-Al metallic systems. As a result, several new BMGs with superior GFA in this system were successfully developed. [doi:10.2320/matertrans.MJ200762]

(Received November 30, 2006; Accepted February 13, 2007; Published August 25, 2007)

Keywords: *bulk metallic glasses, deep eutectics, heat of mixing, zirconium-copper-iron-aluminum system*

1. Introduction

Currently, the synthesis of bulk metallic glasses (BMGs) is the subject of considerable scientific and technological interest because of their promising applications as engineering materials. Good glass-forming compositions in a given system are often at or near "deep" eutectics, as has been clearly demonstrated in many alloy systems.[1–8] For binary systems, it is straightforward to use the eutectic compositions as starting points to explore novel metallic glasses because their phase diagrams are readily available. For multi-component systems, however, it is hard to determine whether they have deep eutectics and where these deep eutectics are located. As a result, the common practice for exploring BMGs in the complex, multi-component metallic systems is to experimentally map out glass-forming ability (GFA) of every single composition, which is unavoidably tedious and time-consuming, and the outcome is always unpredictable. Therefore, a simple strategy for efficiently and effectively designing multicomponent BMGs is necessary.

Up to date, numerous BMG compositions have been discovered and many of them can be treated as a special A-B type binary system by following the constraints elaborated below:

1) Element A can form binary deep eutectics with each B-type element (e.g., B_1, B_2 and B_3). Generally, heat of mixing of the atomic pairs of A-B_1, A-B_2 and A-B_3 is largely negative.
2) The tendency for forming bonding between atomic pairs B_1-B_2, B_1-B_3 and B_2-B_3 is rather weak. Heat of mixing of these pairs is usually near zero, and consequently, the B-type elements tend to form continuous solid solution and/or do not have a strong affinity with each other.

Table 1 lists a few typical multi-component BMG systems that can be reformatted into a A-B_i type binary system as shown in the fourth column of Table 1, together with heat of mixing of all possible binary pairs.[9–20] In order to take advantage of this special categorization, we have recently proposed a basic physical concept of "ideal" glass-forming liquids in which binary eutectics can be treated thermodynamically as basic constituent units.[21] This concept leads to the development of a simple but reliable method for quickly locating glass-forming compositions with superior GFA. As an example, alloy design of BMGs with superior GFA in the Zr-Cu-Fe-Al system will also be demonstrated using the current approach, which will verify our concept and the usefulness of our "shortcut" strategy in return.

2. Theoretic analysis

2.1 Concept of *ideal* glass-forming liquids

Figure 1 schematically shows a composition diagram for a quaternary system consisting of four elements, i.e., A, B_1, B_2 and B_3, which can be regarded as the aforementioned A-B binary system. As can be easily inferred from the assumptions mentioned earlier, this alloy system at the liquid state should have the following thermodynamic characteristics:

1. The tendency for forming chemical clusters (or "ensemble") of A-B_1, A-B_2 and A-B_3 (with specific compositions) is much preferred, and
2. The tendency for forming chemical clusters of B_1-B_2, B_1-B_3 and B_2-B_3 is similar to that of B_1-B_1, B_2-B_2 and B_3-B_3 pairs.

Thus, in such a glass-forming liquid, thermodynamic driving force for chemical clustering between binary atomic pairs A-B_1, A-B_2 and A-B_3 is overwhelmed. Thus, the liquids can be simply treated as a mixture of clusters with binary eutectic compositions.

Glass formation is virtually to retain liquid structure without crystallization during solidification. To avoid the crystallization event and obtain large GFA, all chemical clusters in the liquid should be as stable as possible. In this regard, alloy compositions that can induce the formation of clusters between the same constituent (e.g., the corner compositions in Fig. 1) are not desirable for glass formation because these clusters are extremely unstable and tend to form crystalline phases. Good glass-forming liquids should contain mainly the three types of binary A-B_i clusters and the interaction between these three chemical ensembles is

*Corresponding author, Email: luzp@skl.ustb.edu.cn

Table 1 Typical bulk metallic glasses that can be treated as ideal A-B_i liquids.[9–20] EU, SS and LS represent deep eutectic, continuous solid solution and large solubility, respectively. The digit numbers in brackets indicate heat of mixing ΔH (kJ/mol) between the atomic pair.

Typical BMG System	*A-B* pairs	*B-B* pairs	*Ideal* liquid system A-B_i
Pd-Ni-P[9,10]	Pd-P: EU (−36.5) Ni-P: EU (−34.5)	Pd-Ni: SS (0)	P-(Pd,Ni)
Pd-Ni-Cu-P[9,10]	Cu-P: EU (−17.5)	Cu-Pd: SS (−14) Cu-Ni: SS (+4)	P-(Pd,Cu,Ni)
Pt-Ni-Cu-P[11]	Pt-P: EU (−34.5) Ni-P: EU (−34.5) Cu-P: EU (−17.5)	Pt-Ni: SS(−5) Cu-Pt: SS(−12) Cu-Ni: SS(+4)	P-(Pt,Cu,Ni)
La-Al-Ni[12]	La-Al: EU (−38) La-Ni: EU (−27)	Ni-Al: LS (−22)	La-(Al, Ni)
La-Cu-Al-Ni[13]	La-Cu: EU (−21)	Cu-Ni: SS (+4) Al-Cu: LS(−1)	La-(Cu, Al, Ni)
Cu-Zr-Ti[14]	Cu-Zr: EU(−23) Cu-Ti: EU(−9)	Zr-Ti: SS (0)	Cu-(Zr, Ti)
Y-Co-Al[15]	Y-Co: EU(−22) Y-Al: EU(−38)	Co-Al: LS(−19)	Y-(Co, Al)
Ni-Nb-Ta[16]	Ni-Nb: EU(−30) Ni-Ta: EU(−29)	Nb-Ta: LS(0)	Ni-(Nb,Ta)
Ni-Nb-Ti[16]	Ni-Ti: Eu(−35)	Nb-Ti: SS(2)	Ni-(Nb,Ti)
Zr-Cu-Al[17]	Zr-Cu: EU(−23) Zr-Al: EU(−44)	Al-Cu: LS(−1)	Zr-(Cu,Al)
Zr-Ni-Cu-Al[18,19]	Zr-Ni: Eu(−49)	Al-Ni: LS(−22) Cu-Ni: SS(+4)	Zr-(Ni,Cu,Al)
Cu-Ni-Zr-Ti[20]	Cu-Zr: EU(−23) Cu-Ti: EU(−9) Ni-Zr: EU(−49) Ni-Ti: Eu(−35)	Cu-Ni: SS(+4) Zr-Ti: SS(0)	(Cu,Ni)-(Zr,Ti)
Y-Sc-Co-Al[15]	Y-Co: EU(−22) Y-Al: EU(−38) Sc-Co:EU(−30) Sc-Al: EU(−38)	Y-Sc: SS(+1) Co-Al: LS(−19)	(Y,Sc)-(Co,Al)

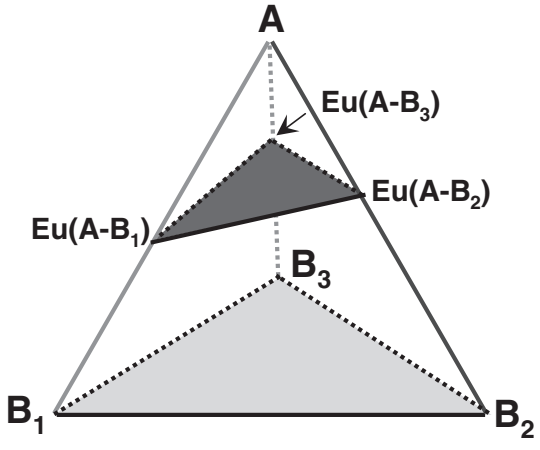

Fig. 1 Composition diagram for a quaternary *ideal* glass-forming liquid A-(B_1,B_2,B_3). Good glass formers in the system are likely within the composition range indicated by the blue triangle plane.

insignificant and negligible (i.e., the cross term between these clusters is minimal) because of the small negative heating of mixing of B-type elements. As such, these three binary clusters can be treated as independent units in considering the stability of these glass-forming liquids in the multi-component A-(B_1,B_2,B_3) system. With reference to ideal solid solution model, we denote such kind of liquids as an "ideal" liquid hereafter.

2.2 Glass formation in the ideal A-(B_1,B_2,B_3) liquids

As demonstrated previously, in order to obtain large GFA, the three major types of binary A-B_i clusters in the ideal A-(B_1,B_2,B_3) liquid should be as stable as possible during solidification. It is well known that the binary eutectics Eu(A-B_i) ($i = 1$, 2 and 3) actually represents the chemical composition of the most stable ensembles in the individual A-B_i binary system. Therefore, good glass-forming liquids C_{am} in the A-(B_1,B_2,B_3) system can be expressed as follows:

$$C_{am} = \alpha[\mathrm{Eu}(A\text{-}B_1)] + \beta[\mathrm{Eu}(A\text{-}B_2)] + \sigma[\mathrm{Eu}(A\text{-}B_3)]. \quad (1)$$

where α, β and σ are related to the percentage of each binary eutectic ensembles, and their sum is the *unity*. It is to be noted that C_{am} actually represents a composition plane bounded by the three different binary eutectics, as indicated by the blue triangle in Fig. 1. As such, the total number of compositions that are needed to be investigated in the ideal A-(B_1,B_2,B_3) system is reduced from a 3-dimenional space to a 2-dimensional plane.

2.3 Basic composition for alloy design in the *ideal* glass-forming liquids

For quickly locating superior glass-formers in the above ideal multicomponent systems, a base composition C_{base} (i.e., the starting point) is required to be first determined. In other words, initial values of mixing constants α, β and σ in eq. (1) has to be determined quickly.

It has been demonstrated that glass formation is a competition between liquid phase and resulting crystalline phases during solidification.[22,23] The tendency for forming crystalline phases from the individual binary clusters is dominated by their concentration and heat of mixing. High concentration and large negative heat of mixing will facilitate the formation of crystalline phases/compounds. In order to retain liquid structure to low temperatures without crystallization, α, β and σ values in eq. (1) have to be determined in a way that clusters with large negative heat of mixing should have relatively low concentration. Thus, the tendency for forming all the crystalline phases can be minimized. As a rule of thumb, therefore, an initial value of α, β and σ for a base composition C_{base} can be derived based on

$$\alpha\Delta H_{A\text{-}B_1} = \beta\Delta H_{A\text{-}B_2} = \sigma\Delta H_{A\text{-}B_3}, \tag{2}$$

where $\Delta H_{A\text{-}B_1}$, $\Delta H_{A\text{-}B_2}$ and $\Delta H_{A\text{-}B_3}$ are heat of mixing for the clusters A-B_1, A-B_2 and A-B_3, respectively. Combining eqs. (1) and (2), one can quickly locate C_{base} for glass formation in the ideal A-(B_1,B_2,B_3) system.

Our concept about the "ideal" liquids has been indirectly confirmed by environmental radial distribution function (RDF) studies in several typical BMGs. For example, anomalous X-ray scattering experimental work has revealed that the environmental radial distribution function (RDF) around Ni in the amorphous $Pd_{40}Cu_{30}Ni_{10}P_{20}$ alloy which can be treated as a binary P-(Pd,Ni,Cu) system based on the constituent binary phase diagrams, and heat of mixing between all binary atomic pairs is nearly same as that in the $Pd_{40}Ni_{40}P_{20}$ alloy.[9] In other words, substituting 30% Ni with Cu has no effect on the atomic distribution and clustering in the undercooled liquid.

Based on binary phase diagrams,[24] Zr forms deep eutectics with Fe, Cu and Al and heating of mixing of the Zr-Fe, Zr-Cu and Zr-Al atomic pair is -25, 23 and -44 kJ/mol, respectively.[25,26] Meantime, Cu, Fe and Al have large mutual solubility with each other[24] and the heat of mixing of Cu-Fe, Cu-Al and Fe-Al is $+13$, -1 and -11 kJ/mol,[25,26] respectively, all of which are much smaller than that of the three strong atomic pairs. As such, the Zr-Fe-Cu-Al alloys can be simplified to an A-B_i type ideal liquid. Next, we will use the Zr-(Fe,Cu,Al) system as an example to further elucidate the proposed strategy and also to demonstrate how new BMGs with superior GFA can be quickly explored with this strategy.

3. Experimental

Alloys were obtained by arc-melting a mixture of commercial-grade metals with purity from 99 to 99.9% in a purified argon atmosphere. The resultant homogeneous alloys were then re-melted onto the top of a copper mold with various diameters in a Ti-gettered, helium atmosphere, and the molten liquids were thus drop-cast into the mold using its own gravity. The samples for X-ray diffraction (XRD) measurements were sliced from as-cast rods by electrical discharging machine and then polished with emery papers. The thermal properties associated with the glass transition, supercooled liquid and crystallization, and melting behavior of these as-cast alloys were examined by a Netzsch model 404 differential scanning calorimeter (DSC) at a heating rate of 20 K/min in a flow of purified argon gas after evacuating to a high vacuum of $\sim 10^{-5}$ Pa. Microstructures of as-cast alloys were also characterized by optical microscopy.

4. Application of the eutectic-pair approach to the Zr-Fe-Cu-Al system

4.1 Base alloys for bulk glass formation

In a generalized case, for a system $(A_1, A_2, \cdots A_n)$-(B_1, $B_2, \cdots B_m$), if all constituent elements can be categorized into two types, i.e, A_i and B_j as discussed earlier, then this system can be considered as ideal liquids and starting compositions for glass formation can be determined quickly based on the knowledge of basic binary systems:

$$C_{\text{am}} = \sum_{i=1}^{m}\sum_{j=1}^{n} C_{ji}(A_jB_i), \tag{3}$$

where A_i ($i = 1, 2, \cdots$ n) are base elements, B_j ($j = 1, 2, \cdots$ m) the glass-forming elements, C_{ij} ($\sum_{j=1}^{m}\sum_{i=1}^{n} C_{ij} = 1$) are the fractions of binary eutectics, A_iB_j is the composition of binary A_i-B_j eutectics with the lowest melting point (in the case where eutectics with similar melting points, line-phases eutectics are preferred), and m and n are the numbers of base elements and glass-forming elements, respectively. The content C_{ij} of eutectic pair A_i-B_j can be initially determined based on the following consideration:

$$C_{ij}\Delta H_{Aj\text{-}Bi} = \text{constant} \tag{4}$$

As elaborated in the previous section, the Zr-Fe-Cu-Al quaternary system can be treated as an ideal A-B_i type liquid as far as the GFA is concerned. Following eqs (3) and (4) in combination with heat of mixing values between different atomic pairs, one can quickly determine the basic glass-forming compositions in the Zr-Fe-Cu-Al system, which can be expressed below:

$$\begin{aligned} C_{\text{base}} &= \alpha[Eu(\text{Zr-Fe})] + \beta[Eu(\text{Zr-Cu})] + \sigma[Eu(\text{Zr-Al})] \\ &= 0.38[Eu(\text{Zr-Fe})] + 0.41[Eu(\text{Zr-Cu})] \\ &\quad + 0.21[Eu(\text{Zr-Al})] \end{aligned} \tag{5}$$

Table 2 shows the selection of the binary eutectic systems and the detailed formula of two based alloys obtained using the above equation, together with the maximum achievable size for fully glassy structures with the traditional copper mold casting technique. Figure 2 exhibits the corresponding XRD patterns of the central part of the as-cast rods of these

Table 2 Base composition C_{base} for glass formation in the Zr-(Fe,Cu,Al) alloy system.

Alloy No.	Glass-forming composition, C_{am}	Basic alloy	D_{max}, mm
Base-1	$0.38(Zr_{76}Fe_{24})+0.41(Zr_{38}Cu_{62})+0.21(Zr_{70}Al_{30})$	$Zr_{59.2}Cu_{25.4}Fe_{9.1}Al_{6.3}$	7
Base-2	$0.38(Zr_{76}Fe_{24})+0.41(Zr_{38}Cu_{62})+0.21(Zr_{51}Al_{49})$	$Zr_{55.2}Cu_{25.4}Fe_{9.1}Al_{10.3}$	7

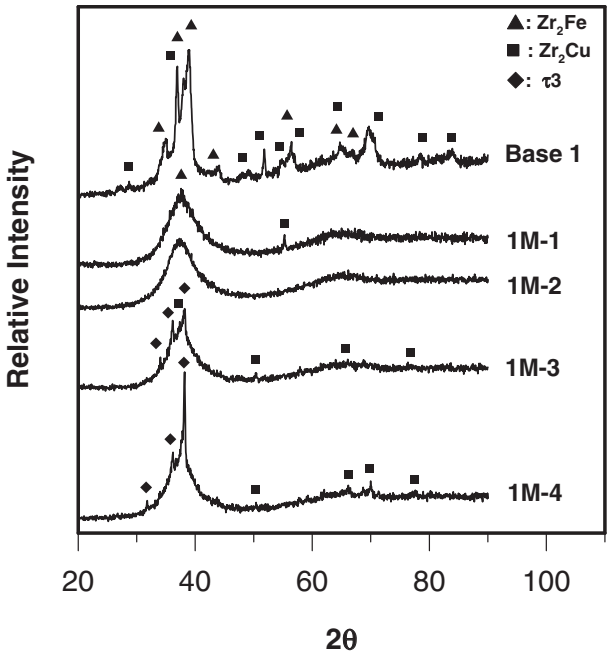

Fig. 2 XRD patterns of the center of the cross section of the two based alloys with diameters of 7 and 10 mm.

base alloys. As can be seen, only two diffuse humps were observed for both alloys Base-1 and Base-2 with a diameter of 7 mm, indicating that these samples are mostly amorphous. For the as-cast samples with a larger diameter of 10 mm, however, sharp crystalline peaks corresponding to ZrCu and Zr_2Cu phases were detected for the Base-1 while Zr_2Cu and Zr_2Fe phases were appeared for the Base-2. These XRD measurements are consistent with optical micrographs of the cross-section of these samples as shown in Fig. 3. Different morphologies of the crystalline phases embedded in the amorphous matrix were observed. It appears to be that both alloys underwent a peritectic reaction upon cooling and outer part of the crystalline phases is different from its inner. Our experimental results suggest that the maximum attainable diameter for a fully glassy structure in these base alloys is at least 7 mm with the conventional copper mold casting technique. It is important to point out that the selection of the binary eutectic $Zr_{70}Al_{30}$ and $Zr_{51}Al_{49}$ for the Zr-Al atomic pair yields similar GFA. According to the Zr-Al binary phase diagram,[24] the melting point of the eutectic $Zr_{51}Al_{49}$ is 1485 °C, 135 °C higher than that of the "deepest" eutectic $Zr_{70}Al_{30}$. Nevertheless, the eutectic $Zr_{51}Al_{49}$ consists of two line-compounds Zr_2Al_3 and Zr_4Al_3 with no mutual solubility, whilst the "deepest" eutectic $Zr_{70}Al_{30}$ consists of Zr_5Al_3 and β–Zr that can dissolve a large quantity of Al. As mentioned previously, GFA is related not only to the liquid phase stability but also the resistance to crystallization.[22,23] From the standpoint of the liquid phase stability, binary eutectics with the lowest melting point is preferred, whilst from the standpoint of crystallization resistance, binary eutectics consisting of line-compounds with strict stoichiometry should retard the formation of crystalline phase because the long-range diffusion is required for crystallization, and thus favor glass formation. The overall effects from binary eutectics are always related to two aspects, i.e., the melting temperature and the constituent components. In the current case, binary eutectic $Zr_{51}Al_{49}$ kinetically favors glass formation but $Zr_{70}Al_{30}$ is thermodynamically preferred. Nevertheless, in the case where aluminum also has relatively strong bonding with other B-type elements (e.g., Ni in the Zr-Ni-Cu-Al system[21]), selection of high Al-containing eutectic $Zr_{51}Al_{49}$ may not be feasible because high Al content may induce the formation of crystalline phases from the B-B type atomic pairs.

4.2 Further improvement of GFA: fine tuning the mixing constants

Once the starting compositions are determined, their GFA can be further improved by fine tuning the mixing constants α, β and σ based on the formation of crystalline phases (see Fig. 3). As an example, here we will simply demonstrate how superior glass formers around the first base alloy can be located via fine-tuning the mixing constants in eq. (5). As discussed above (Figs. 2 and 3), crystalline phases of Zr_2Fe and Zr_2Cu were formed in the alloy base-1 with a diameter of 10 mm, suggesting that both α and β values in eq. (5) should be decreased so that the concentration of Zr-Fe and Zr-Cu atomic pairs could be reduced and formation of Zr_2Fe and Zr_2Cu can thus be suppressed. Therefore, glass formation in alloys with gradually decreased α and β values (the σ would increase accordingly) were subsequently studied as shown in Table 3. It is to be noticed that, as α and β values are decreased, Zr contents actually remain constant while Cu and Fe contents are decreased with the consequent increase of Al concentration in the resultant alloys. Figure 4 shows the XRD patterns of the cross-section of as-cast, 10 mm rods for all modified alloys. For the alloy 1M-1 ($\alpha = 0.37$, $\beta = 0.40$ and $\sigma = 0.23$), small crystalline peaks corresponding to Zr_2Fe and Zr_2Cu superimposed on two typical amorphous humps is seen, indicating that the GFA of this alloy is much improved as compared with that of the base alloy, although the primary phases are still the same. With the further decrease of α and β values (i.e., alloy 1M-2 wiht $\alpha = 0.36$, $\beta = 0.39$ and $\sigma = 0.25$), a fully amorphous structure is obtained. With the excessive decrease of α and β values (i.e., alloys 1M-3 and 1M-4), however, a new Zr-Cu-Al ternary crystalline phase (i.e., $\tau 3$), along with Zr_2Cu, is appeared on the XRD patterns, revealing that the GFA of these alloys is deteriorated because of the rapid formation of these new primary phases. Detailed phase competition as a function of the mixing constants and compositions is also summarized in

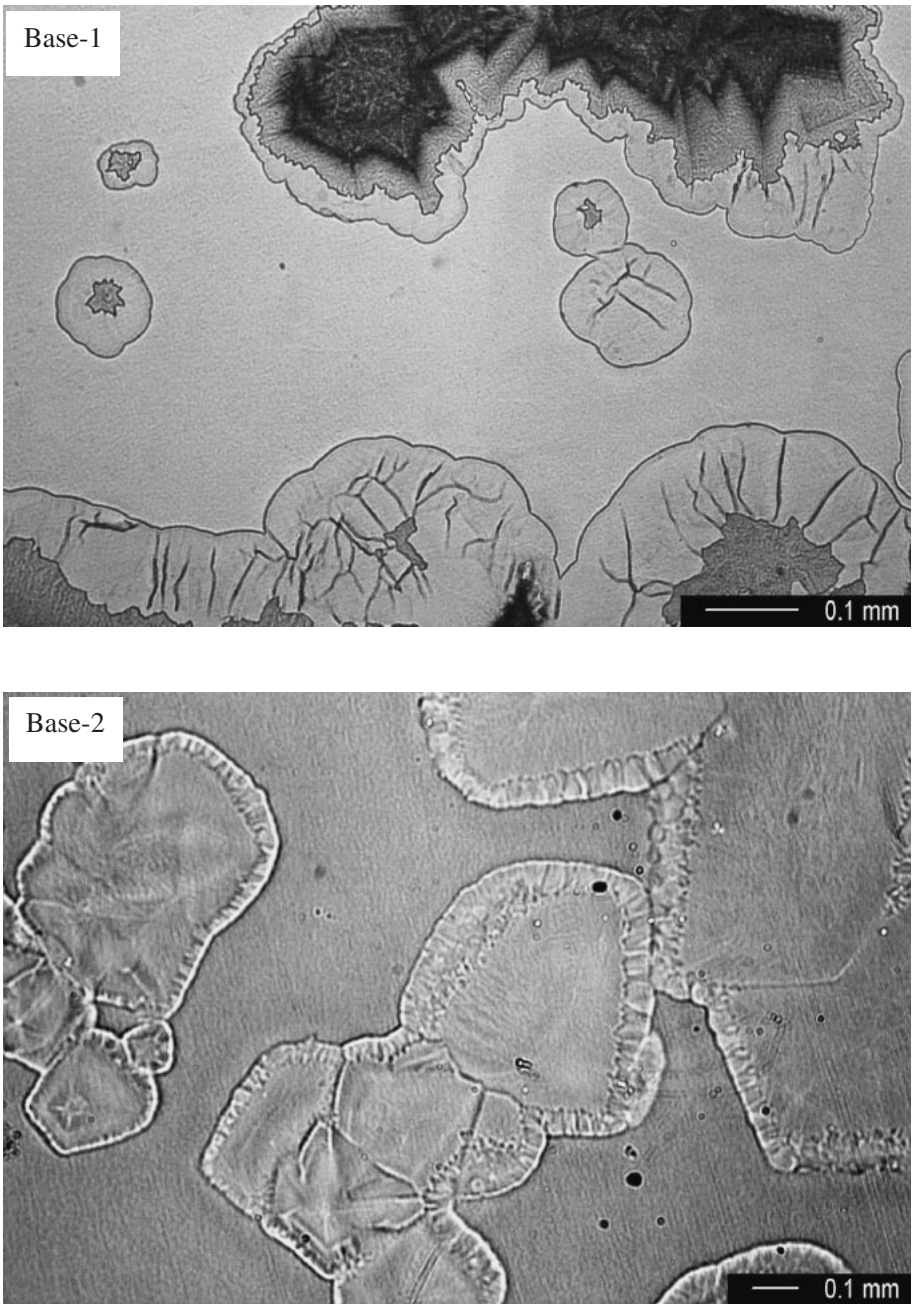

Fig. 3 Optical micrographs for as cast, 10 mm rods of the base alloys. (a) alloy Base-1 and (b) alloy Base-2.

Table 3 Composition refinement for glass formation around the first base composition $Zr_{59.2}Cu_{25.4}Fe_{9.1}Al_{6.3}$ in the Zr-(Fe,Cu,Al) system. The castings were carried out under argon atmosphere with a mold diameter of 10 mm.

Alloy No.	Adjustment of mixing constants	Composition	Major Primary phases
Base-1	$0.38(Zr_{76}Fe_{24})+0.41(Zr_{38}Cu_{62})+0.21(Zr_{70}Al_{30})$	$Zr_{59.2}Fe_{9.1}Cu_{25.4}Al_{6.3}$	Zr_2Cu+Zr_2Fe
1M-1	$0.37(Zr_{76}Fe_{24})+0.40(Zr_{38}Cu_{62})+0.23(Zr_{70}Al_{30})$	$Zr_{59.2}Fe_{8.9}Cu_{24.8}Al_{6.9}$	Zr_2Cu+Zr_2Fe
1M-2	$0.36(Zr_{76}Fe_{24})+0.39(Zr_{38}Cu_{62})+0.25(Zr_{70}Al_{30})$	$Zr_{59.2}Fe_{8.6}Cu_{24.2}Al_{7.5}$	Amorphous
1M-3	$0.35(Zr_{76}Fe_{24})+0.38(Zr_{38}Cu_{62})+0.27(Zr_{70}Al_{30})$	$Zr_{59.2}Fe_{8.4}Cu_{23.6}Al_{8.1}$	$Zr_2Cu+\tau 3$
1M-4	$0.34(Zr_{76}Fe_{24})+0.37(Zr_{38}Cu_{62})+0.29(Zr_{70}Al_{30})$	$Zr_{59.2}Fe_{8.2}Cu_{22.9}Al_{8.7}$	$Zr_2Cu+\tau 3$

Table 3. As indicated in the table, optimum values of α, β and σ are obtained in the alloy 1M-2 (i.e., $Zr_{59.2}Fe_{8.6}Cu_{24.2}Al_{7.5}$) which is a superior glass former around the first base alloy. Similarly, another superior glass former (i.e., $Zr_{55.4}Cu_{24.2}Fe_{9.1}Al_{11.3}$) around the alloy Base-2 can also be located with the same approach.

In order to further understand glass formation in alloys with different mixing constants, DSC measurements were conducted and the results are given in Fig. 5 which shows glass transition, crystallization and melting behavior of all

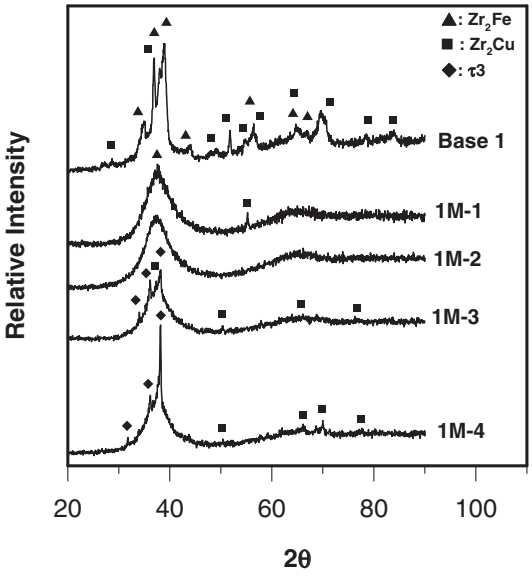

Fig. 4 XRD patterns of the center of the cross section of all modified alloys with a diameter of 10 mm.

the modified alloys in comparison with those of the base alloy. A summary of characteristic temperatures (Note that fully amorphous rods with a diameter of 1.2 mm were used for the measurement of T_g and T_x), thermal stability ΔT and calculated GFA indicators T_{rg} and γ were given in Table 4. As can be seen from Fig. 5(a) and Table 4, both glass transition temperature T_g and onset crystallization temperature T_x show a maximum value in the optimum alloy 1M-2, and alloys with higher Al content (i.e., higher σ value) generally have a higher T_g and T_x. From Fig. 5(b) and Table 4, it is obvious that the onset melting temperature (i.e., solidus temperature) almost unchanged for all alloys investigated, implying that these alloys are associated with the same eutectic point. Nevertheless, the off-set melting point T_l (i.e., liquidus temperature) is monotonously decreased with the increase of Al concentration in the alloys, which may be originated from the low melting point of the constituent element Al. Supercooled liquid region ΔT of all modified alloys are higher than that of the base alloy and reach the maximum value of 98 K in the optimum alloy, suggesting that these amorphous alloys have quite large thermal stability. The GFA indicator T_{rg}, calculated by T_g/T_l,[27] correctly shows the largest value for the best alloy 1M-2 but can not effectively represent the GFA of high Al-containing alloys 1M-3 and 1M-4. The γ parameter, defined as $T_x/(T_g + T_l)$, correlated well with GFA for all alloys and the largest γ value for the best glass former is originated from the abrupt increase in the onset crystallization temperature T_x. Based on the definition of the γ parameter,[22,23] this observation reflects that decrease of the concentration of the Zr-Fe and Zr-Cu atomic pairs in this specific base alloy greatly enhance the crystallization resistance in the resulting alloys, thus consequently leading to larger GFA. The above observation is different from what we reported previously about the effects of yttrium additions on GFA of the Fe-based alloys in which the optimum GFA is dictated by the low liquidus temperature. In other words, the GFA enhancement is mainly originated from the larger liquid phase stability.[28]

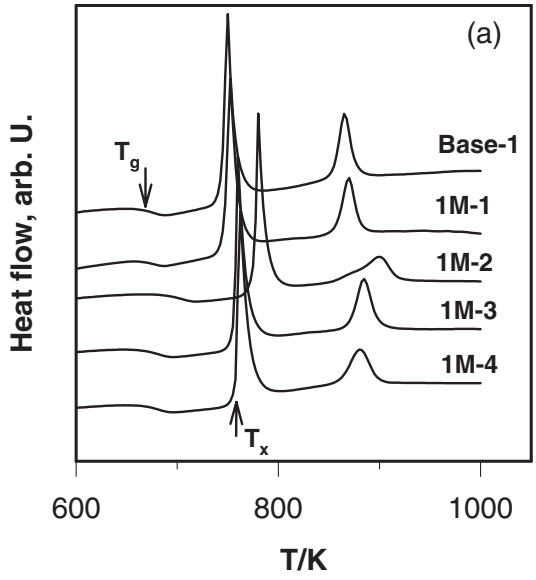

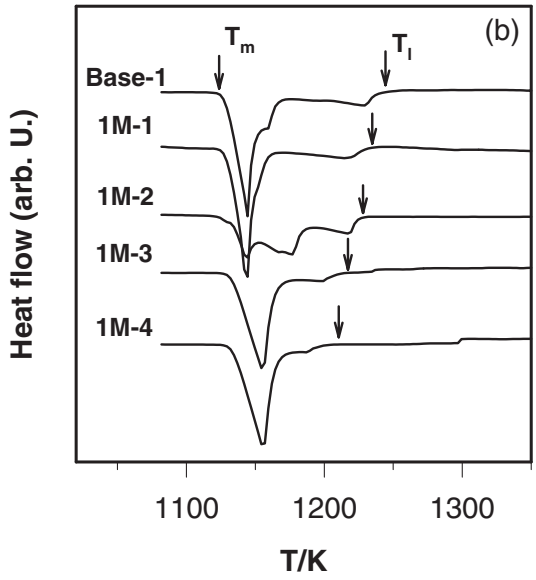

Fig. 5 DSC heating curves of all modified alloys with various α, β and σ values at a rate of 20 K/min.

Table 4 Characteristic temperatures including glass transition temperature T_g, onset crystallization temperature T_x, onset melting temperature T_m, and liquidus temperature T_l, together with calculated ΔT, γ and T_{rg} value for all modified alloys around the first base alloy.

Alloy No.	T_g	T_x	T_m	T_l	γ	T_{rg}	ΔT
Base-1	661	745	1130	1238	0.392	0.534	84
1M-1	658	747	1132	1231	0.395	0.535	89
1M-2	679	777	1134	1223	0.409	0.555	98
1M-3	667	757	1133	1206	0.404	0.553	90
1M-4	667	759	1134	1201	0.406	0.555	92

5. Conclusions

A physical concept of the *ideal* glass-forming liquid has been proposed, which leads to the construction of a simple but reliable method useful for identifying bulk glass-forming compositions in multi-component systems using binary

eutectic as composition unit rather than individual elements. As an example, the current method was applied to the Zr-Fe-Cu-Al systems and bulk glass formation in this specific system was studied in details. As a result, several new BMGs with superior GFA were successfully developed using the method, and DSC measurements reveal that the GFA increase in the best alloys is due to the large enhancement of crystallization resistance. In return, verification work in the Zr-Fe-Cu-Al system confirms the reliability and usefulness of the current strategy.

Acknowledgements

This research was sponsored in part by the Division of Materials Sciences and Engineering, Office of Basic Energy Sciences, U.S. Department of Energy under contract DE-AC05-00OR-22725 with UT-Battelle, LLC.

REFERENCES

1) N. Nishiyama and A. Inoue: Appl. Phys. Lett. **80** (2002) 568–570.
2) H. Choi-Y, D. H. Xu and W. L. Johnson: Appl. Phys. Lett. **82** (2003) 1030–1032.
3) H. W. Kui, A. L. Greer and D. Turnbull: Appl. Phys. Lett. **45** (1984) 615–616.
4) M. H. Cohen and D. Turnbull: Nature **189** (1961) 131–132.
5) W. H. Wang, J. J. Lewandowski and A. L. Greer: J. Mater. Res. **20** (2005) 2307–2313.
6) Z. P. Lu, C. T. Liu and W. D. Porter: Appl. Phys. Lett. **83** (2003) 2581–2583.
7) Z. P. Lu, C. T. Liu, J. R. Thomson and W. D. Porter: Phys. Rev. Lett. **92** (2004) 245503.
8) D. Ma, H. Tan, D. Wang, Y. Li and E. Ma: Appl. Phys. Lett. **86** (2005) 191906.
9) A. Inoue: Acta Mater. **48** (2000) 279–306.
10) A. L. Drehman, A. L. Greer and D. Turnbull: Appl. Phys. Lett. **41** (1982) 716–717.
11) J. Schroers and W. L. Johnson: Appl. Phys. Lett. **84** (2004) 3666–3669.
12) A. Inoue, T. Nakamura, T. Sugita, T. Zhang and T. Masumoto: Mater. Trans. JIM **34** (1993) 351–358.
13) H. Tan, Y. Zhang, D. Ma, Y. P. Feng and Y. Li: Acta Mater. **51** (2003) 4551–4561.
14) A. Inoue, W. Zhang, T. Zhang and K. Kurosaka: Acta Mater. **49** (2001) 2645–2652.
15) F. Q. Guo, S. J. Poon and G. J. Shiflet: Appl. Phys. Letts. **83** (2003) 2575–2577.
16) M. H. Lee, J. Y. Lee, D. H. Bae, W. T. Kim, D. J. Sordelet and D. H. Kim: Intermetallics **12** (2004) 1133–1137.
17) Y. Yokoyama, K. Fukaura and A. Inoue: Mater. Sci. Engi. A **375–377** (2004) 427–431.
18) A. Inoue and T. Zhang: Mater. Trans. JIM **37** (1996) 185–187.
19) A. Inoue, Y. Yokoyama, Y. Shinohara and T. Masumoto: Mater. Trans. JIM **35** (1994) 923–926.
20) X. H. Lin and W. L. Johnson: J. Appl. Phys. **78** (1995) 6514–6519.
21) Z. P. Lu, J. Shen, D. W. Xing, J. F. Sun and C. T. Liu: Appl. Phys. Letts. **89** (2006) 071910.
22) Z. P. Lu and C. T. Liu: Phys. Rev. Lett. **91** (2003) 115505.
23) Z. P. Lu, and C. T. Liu: Intermetallics **12** (2004) 1035–1043.
24) T. B. Massalski, J. L. Murray, L. H. Bennett, H. Baker and L. Kacprzak: *Binary alloy phase diagrams* (American Society for Metals, Metal Park, Ohio, 1986).
25) F. R. de Boer, R. Boom, W. C. M. Mattens, A. R. Miedema and A. K. Niessen: *Cohesion in Metals*, (North-Holland, Amsterdam, 1988).
26) A. Takeuchi and A. Inoue: Mater. Trans. JIM **41** (2000) 1372–1378.
27) Z. P. Lu, H. Tan, Y. Li and S. C. Ng: Scripta Mater. **42** (2002) 667–673.
28) Z. P. Lu, C. T. Liu, C. A. Carmicheal, W. D. Porter and S. C. Deevi: J. Mater. Res. **19** (2004) 921–929.